NATIONAL ADVISORY COMMITTEE FOR AERONAUTICS

TECHNICAL NOTE

No. 1662

AERODYNAMIC PROPERTIES OF SLENDER WING-BODY COMBINATIONS AT SUBSONIC, TRANSONIC, AND SUPERSONIC SPEEDS

By John R. Spreiter

Ames Aeronautical Laboratory
Moffett Field, Calif.

WASHINGTON

July 1948

NATIONAL ADVISORY COMMITTEE FOR AERONAUTICS

TECHNICAL NOTE NO. 1662

AERODYNAMIC PROPERTIES OF SLENDER WING-BODY COMBINATIONS AT SUBSONIC, TRANSONIC, AND SUPERSONIC SPEEDS

By John R. Spreiter

SUMMARY

A method based on assumptions similar to those of Munk's airship theory and R.T. Jones' low-aspect-ratio pointed-wing theory has been developed to determine simple closed expressions for the load distribution, lift, pitching moment, and center-of-pressure position of inclined slender wing-body configurations having flat-plate wings extending along the continuation of the horizontal diameters of circular fuselage sections. Expressions for the aerodynamic properties of triangular wings in combination with conical bodies, semi-infinite cylindrical bodies, and bodies pointed at the nose but cylindrical at the wing root have been developed in detail for all ratios of body diameter to wing span. In all cases, the lift-curve slope of the wing-body combination was less than that of the wing alone. For the case of the triangular wing and the body pointed at the nose but cylindrical at the wing root, the loss in lift-curve slope reached a maximum of 25 percent at the large diameter-span ratio of 0.707. With a conical body mounted on the same wing, the maximum loss of lift-curve slope was only about 8 percent and occurred at about the same diameter-span ratio.

It is shown that the results are applicable at subsonic and transonic speeds, and at supersonic speeds, provided the entire wing-body combination lies near the center of the Mach cone. Furthermore, it is pointed out that the assumptions related to the study of low-aspect-ratio pointed bodies and the study of moderate-aspect-ratio pointed bodies traveling at sonic speed both lead from Prandtl's linearized equation for compressible flow to the two-dimensional Laplace's equation in the transverse plane although by different means.

The determination of the potential distribution for an inclined moderate-aspect-ratio wing at sonic speed is therefore mathematically equivalent to the determination of the potential distribution for an inclined low-aspect-ratio wing in an incompressible fluid.

INTRODUCTION

In the quest for airplane configurations having aerodynamic properties favorable for supersonic flight, one of the more promising configurations involves the use of a low-aspect-ratio wing. When the general layout of such an airplane is considered, however, comparatively large fuselages are often found necessary. It thus becomes important to study the aerodynamics of a complete wing-body combination throughout the entire Mach number range of the airplane. In an incompressible medium, the mutual interference of a fuselage and wing of high-aspect ratio (to which lifting-line theory is applicable) has been treated by Lennertz, Wieselsberger, Pepper, and Multhopp in references 1, 2, 3, and 4. It is the purpose of this note to treat the effect on the aerodynamic loading of the mutual interference between a low-aspect-ratio pointed wing and a fuselage consisting of a slender body of revolution.

The aerodynamic properties of slender wing-body configurations may be approximated by the method originally used by Munk in studying the aerodynamics of slender airships (reference 5). R. T. Jones (reference 6) applied this method to the study of low-aspect-ratio pointed wings and Ribner (reference 7) extended it to determine the stability derivatives of low-aspect-ratio triangular wings. The essential point in the study of slender bodies by this method is the fact that the flow is approximately two-dimensional when viewed in planes perpendicular to the direction of motion. Methods of classical hydrodynamics may then be employed to determine the load distribution, lift, and center of pressure.

It has been shown by Tsien, Laitone, and R. T. Jones (references 8, 9, and 6) that the aerodynamic properties of very slender bodies of revolution and low-aspect-ratio wings at small angles of attack are unaffected by compressibility at subsonic and supersonic speeds. A similar result will be shown for slender wing-body combinations.

SYMBOLS

A aspect ratio $\left(\frac{4s_{max}^2}{S}\right)$

B	cross-section area of body of revolution (πa^2)
B_b	cross-section area of base of body of revolution
B_m	mean cross section of body of revolution $\left(\frac{\text{volume}}{\text{length}}\right)$
C_L	lift coefficient $\left(\frac{L}{qS}\right)$
C_{L_α}	lift-curve slope $\left(\frac{dC_L}{d\alpha}\right)$
C_{L_W}	lift coefficient of wing without body
C_m	pitching moment coefficient $\left(\frac{M}{qSc}\right)$
C_{m_W}	pitching moment coefficient of wing without body
L	lift
M	pitching moment about apex of wing
M_o	free-stream Mach number
S	wing area
U	velocity of flight
W	complex potential function $(\varphi + i\psi)$
X	complex variable $(y + iz)$
a	radius of body
c	maximum wing chord
c'	distance from apex to section of maximum span
d	semispan of flat plate
l	over-all length of wing-body combination
m	additional apparent mass of circular cylinder

p	static pressure
q	free-stream dynamic pressure
r,θ	polar coordinates
s	local semispan
s_{max}	maximum semispan
t	time
v,w	velocities in y and z directions
x,y,z	Cartesian coordinates
$x_{c.p.}$	distance from apex to center of pressure
φ	velocity potential
ψ	stream function
α	angle of attack
ϵ	downwash angle
η,ζ	transformed rectangular coordinates
ξ	complex variable $(\eta+i\zeta)$
ρ	density of air

Subscripts

W	wing
F	body
c	compressible
i	incompressible

ANALYSIS

General

The flow around an inclined wing–body combination of very low aspect ratio may be approximated by considering it to be two dimensional in transverse planes (perpendicular to the fuselage center line). It can be shown as a consequence of this assumption that the flow in each transverse plane is independent of that in the adjacent planes. Consider a coordinate system moving downward through the air with a velocity $U\alpha$. The wing–body combination is now considered to be flying in the negative x–direction with a velocity U and angle of attack α so that the fuselage center line coincides with the x–axis of the coordinate system and the plane of the wing coincides with the $z = 0$ plane. (See fig. 1(a).) The flow pattern, then, in the arbitrary $x = x_0$ plane during the time of the passage of the wing–body combination is approximately similar to that of the transverse flow around an infinite cylinder having a cross section similar to the local wing–body section. Observed in this plane, the semispan of the wing and the radius of the fuselage change with time as the wing–body combination moves through the plane. The resulting unsteady nature of the flow pattern produces pressure differences between corresponding points on the upper and lower surfaces of the wing and fuselage. The following analysis, therefore, consists of three parts: determination of the velocity potential for the two–dimensional flow around the wing–body sections, determination of the distribution of load over each section, and integration of the loading to determine the total lift and pitching moment. Several examples are included presenting the total lift, center of pressure, and load distribution for typical complete wing–body configurations.

Velocity Potential

It is necessary for the subsequent analysis to know the velocity potential for the unsteady two–dimensional transverse flow field around an infinite cylinder, the cross section of which is varying with time in such a manner that it always remains similar to the wing–body section in the $x = x_0$ plane. Due to the infinite rate of pressure propagation in an incompressible fluid, the study of the unsteady flow of an incompressible fluid is greatly simplified since the flow field at any instant is identical to that of the corresponding steady–state flow. The first step in the solution of the present problem, therefore, is to determine the velocity potential for the steady–state flow around an infinite cylinder having a cross section similar to the wing–body section. In this analysis, only wing–body

configurations having circular fuselage sections and flat-plate wings extending along the extension of a diameter will be treated. The flow around such a section may be obtained from the transverse flow around an infinitely long flat plate by application of the principles of conformal mapping using the Joukowski transformation. Thus we consider the mapping shown in figure 1 in which the ξ plane will be mapped onto the X plane by the relation

$$\xi = X + \frac{a^2}{X} \tag{1}$$

where

$$\xi = \eta + i\zeta$$

and

$$X = y + iz$$

The complex potential function for the flow in the ξ plane is (see, for instance, reference 10)

$$W' = \varphi' + i\psi' = -iU\alpha \sqrt{\xi^2 - d^2} \tag{2}$$

where the primed symbols indicate values in the ξ plane as opposed to the X plane. It is also shown in reference 10 that, if $d=2a$, the flow around a flat plate expressed by equation (2) transforms by equation (1) into the vertical flow around a circle of radius a having its center at the origin. If d is taken larger than $2a$, the flat-plate flow transforms into the desired vertical flow around a cylinder consisting of a circular cylinder of radius a with thin flat plates extending outward along the extension of the horizontal diameter to a distance s from the origin. When the ξ plane is transformed into the X plane in this manner, the complex potential for the flow in the X plane is found to be

$$W = \varphi + i\psi = -iU\alpha \sqrt{\left(X + \frac{a^2}{X}\right)^2 - d^2} = -iU\alpha \sqrt{\left(X + \frac{a^2}{X}\right)^2 - \left(s + \frac{a^2}{s}\right)^2} \tag{3}$$

since the point d in the ξ plane corresponds to the point s in the X plane. The velocity potential φ for the flow in the X plane may

then be found by squaring equation (3), substituting $X = r(\cos\theta + i\sin\theta)$, and solving. Thus is obtained

$$\varphi = \pm \frac{U\alpha}{\sqrt{2}} \sqrt{\left[-\left(1+\frac{a^4}{r^4}\right) r^2 \cos 2\theta + s^2\left(1+\frac{a^4}{s^4}\right) \right] + \sqrt{r^4\left(1+\frac{a^8}{r^8}\right) + 2a^4\cos 4\theta + s^4\left(1+\frac{a^4}{s^4}\right)^2 - 2s^2\left(1+\frac{a^4}{s^4}\right)\left(1+\frac{a^4}{r^4}\right) r^2\cos 2\theta}} \tag{4}$$

where the sign is positive in the upper half plane $(0<\theta<\pi)$ and negative in the lower half plane $(\pi<\theta<2\pi)$.

Load Distribution

Once the velocity potential of a flow field is known, the methods of classical hydrodynamics may be applied to determine the pressure at any point in the field. Consider again, the case shown in figure 1 where the wing-body combination is piercing the $x=x_0$ plane. As previously noted, the flow in the $x=x_0$ plane is considered to be similar to the two-dimensional flow surrounding an infinitely long cylinder having the shape of the wing-body cross section intersected by the $x=x_0$ plane. If the radius of the body a and the semispan of the wing s are considered to be functions of time, equation (4) may be thought of as representing the velocity potential of the unsteady flow in the $x=x_0$ plane. In the case of unsteady two-dimensional potential flow of an incompressible fluid, the pressure at any point fixed in the coordinate system is given by (see, for instance, reference 11, p. 19)

$$-\frac{p}{\rho} = \frac{\partial\varphi}{\partial t} + \frac{1}{2}(v^2+w^2) + F(t) \tag{5}$$

It may be seen that this expression reduces to the well-known Bernouli's equation for the pressure in a steady flow field when the velocity potential is invariant with time $\frac{\partial\varphi}{\partial t} = 0$ and the arbitrary function of time $F(t)$ is a constant.

For any two corresponding points P_1 and P_2 (fig. 1(b)), so selected that $y_1 = y_2$ and $z_1 = -z_2$, the differential pressure at any instant is given by

$$\frac{\Delta p}{\rho} = \frac{p_2 - p_1}{\rho} = -\frac{\partial \varphi_2}{\partial t} + \frac{\partial \varphi_1}{\partial t} - \frac{1}{2}(v_2^2 + w_2^2) + \frac{1}{2}(v_1^2 + w_1^2)$$

$$= +2\frac{\partial \varphi_1}{\partial t} - \frac{1}{2}(v_2^2 + w_2^2) + \frac{1}{2}(v_1^2 + w_1^2) \tag{6}$$

since $-\frac{\partial \varphi_2}{\partial t} = \frac{\partial \varphi_1}{\partial t}$ by reason of symmetry of the flow field. Now if the points are brought to the wing-body surface

$$v_2^2 + w_2^2 = v_1^2 + w_1^2$$

the differential pressure between any two corresponding points (or the loading) is given by

$$\frac{\Delta p}{\rho} = +2\frac{\partial \varphi_1}{\partial t} \tag{7}$$

Utilizing the relationship

$$\frac{\partial \varphi_1}{\partial t} = \frac{\partial \varphi_1}{\partial x}\frac{dx}{dt} = \frac{\partial \varphi_1}{\partial x} U \tag{8}$$

and dividing equation (7) by $\frac{1}{2}U^2$, the loading coefficient is found to be

$$\frac{\Delta p}{q} = \frac{p_l - p_u}{q} = \frac{4\frac{\partial \varphi_1}{\partial x}}{U} = \frac{4}{U}\left(\frac{\partial \varphi_1}{\partial s}\frac{ds}{dx} + \frac{\partial \varphi_1}{\partial a}\frac{da}{dx}\right) \tag{9}$$

The load distribution may now be obtained by substituting the expression for the velocity potential given in equation (4) into equation (9) and letting $\theta=0$ or $\theta=\pi$ for the wing loading and $r=a$ for the fuselage loading. The loading over the wing is then found to be given by

$$\left(\frac{\Delta p}{q}\right)_W = 4\alpha \left\{ \frac{\frac{ds}{dx}\left(1 - \frac{a^4}{s^4}\right) + \frac{da}{dx}\left[2\,\frac{a}{s}\left(\frac{a^2}{s^2} - \frac{a^2}{r^2}\right)\right]}{\sqrt{\left(1 + \frac{a^4}{s^4}\right) - \frac{r^2}{s^2}\left(1 + \frac{a^4}{r^4}\right)}} \right\} \tag{10}$$

and that over the fuselage is given by

$$\left(\frac{\Delta p}{q}\right)_F = 4\alpha \left\{ \frac{\frac{ds}{dx}\left(1 - \frac{a^4}{s^4}\right) + \frac{da}{dx}\left[2\,\frac{a}{s}\left(\frac{a^2}{s^2} - \cos 2\theta\right)\right]}{\sqrt{\left(1 + \frac{a^4}{s^4}\right) - 2\,\frac{a^2}{s^2}\cos 2\theta}} \right\} \tag{11}$$

In Cartesian coordinates, the loading over the fuselage is

$$\left(\frac{\Delta p}{q}\right)_F = 4\alpha \left[\frac{\frac{ds}{dx}\left(1 - \frac{a^4}{s^4}\right) + 2\,\frac{a}{s}\,\frac{da}{dx}\left(1 + \frac{a^2}{s^2} - 2\,\frac{y^2}{a^2}\right)}{\sqrt{\left(1 + \frac{a^2}{s^2}\right)^2 - 4\left(\frac{y^2}{s^2}\right)}} \right] \tag{12}$$

Total Lift and Moment

The total lift and pitching moment of a complete wing-body combination may be determined by integrating the loading over the entire plan-form area. It is convenient to carry out the integration by first evaluating the lift on one spanwise strip and then integrating these elemental lift forces over the length of the wing-body combination. The lift on a spanwise strip of width dx is given by

$$dL = 2q\,dx\left[\int_0^{\frac{\pi}{2}} \left(\frac{\Delta p}{q}\right)_F a \sin\theta\, d\theta + \int_a^s \left(\frac{\Delta p}{q}\right)_W dr \right] \tag{13}$$

or, in Cartesian coordinates

$$dL = 2q\,dx\left[\int_0^a \left(\frac{\Delta p}{q}\right)_F dy + \int_a^s \left(\frac{\Delta p}{q}\right)_W dy \right] \tag{14}$$

When the indicated operations are performed, the following expressions for the elemental lift on the wing and body are obtained.

$$\frac{d}{dx}\left(\frac{L}{q}\right)_F = 4\alpha s\left[\left\{\frac{ds}{dx}\left(1-\frac{a^4}{s^4}\right)+\frac{da}{dx}\left(1-\frac{a^2}{s^2}\right)+\frac{da}{dx}\left[2\frac{a}{s}\left(1+\frac{a^2}{s^2}\right)-\frac{s}{2a}\left(1+\frac{a^2}{s^2}\right)^2\right]\right\}\sin^{-1}\frac{2\frac{a}{s}}{1+\frac{a^2}{s^2}}\right] \tag{15a}$$

$$\frac{d}{dx}\left(\frac{L}{q}\right)_W = 2\pi\alpha s\left\{\frac{ds}{dx}\left(1-\frac{a^4}{s^4}\right)-\frac{da}{dx}\left[2\frac{a}{s}\left(1-\frac{a^2}{s^2}\right)\right]\right\}+4\alpha s\left\{\frac{ds}{dx}\left(1-\frac{a^4}{s^4}\right)+\frac{da}{dx}\left[2\frac{a}{s}\left(1+\frac{a^2}{s^2}\right)\right]\right\}\sin^{-1}\frac{1-\frac{a^2}{s^2}}{1+\frac{a^2}{s^2}} \tag{15b}$$

Noting that

$$\sin^{-1}\frac{2\frac{a}{s}}{1+\frac{a^2}{s^2}}+\sin^{-1}\frac{1-\frac{a^2}{s^2}}{1+\frac{a^2}{s^2}}=\frac{\pi}{2} \tag{16}$$

equations (15a) and (15b) may be combined and simplified to give the following expression for the total lift on an elemental spanwise strip.

$$\frac{d}{dx}\left(\frac{L}{q}\right) = 4\pi\alpha s\left[\frac{ds}{dx}\left(1-\frac{a^4}{s^4}\right)+\frac{da}{dx}\left(2\frac{a^3}{s^3}\right)\right]$$

$$+ 2\alpha s\frac{da}{dx}\left[2\left(1-\frac{a^2}{s^2}\right)-\frac{s}{a}\left(1+\frac{a^2}{s^2}\right)^2 \sin^{-1}\frac{2\frac{a}{s}}{1+\frac{a^2}{s^2}}\right] \quad (17)$$

The lift, pitching moment, and center of pressure of the complete wing-body combination may now be determined by integration of the lift of all the elemental strips

$$L = q\int\frac{d}{dx}\left(\frac{L}{q}\right)dx \quad (18)$$

$$M = -q\int x\frac{d}{dx}\left(\frac{L}{q}\right)dx \quad (19)$$

$$x_{c.p.} = -\frac{M}{L} \quad (20)$$

where the integration interval extends from the most forward point to the most rearward point of the wing-body configuration. The lift coefficient, moment coefficient, and center of pressure may be determined from equations (18), (19), and (20) by division by appropriate constants

$$C_L = \frac{1}{S}\int\frac{d}{dx}\left(\frac{L}{q}\right)dx \quad (21)$$

$$C_m = -\frac{1}{Sc}\int x\frac{d}{dx}\left(\frac{L}{q}\right)dx \quad (22)$$

$$\frac{x_{c.p.}}{c} = -\frac{C_m}{C_L} \quad (23)$$

where S is the reference area and c the reference chord or length.

Effect of Compressibility

In contrast to the well-known infinite-aspect-ratio case where the pressures on the surface of a wing are influenced by compressibility in a manner described by the Prandtl-Glauert relation, it has been shown by several investigators that the pressures on very low-aspect-ratio wings and very slender bodies of revolution are unaffected by compressibility. This result has been found by Jones (reference 6) for low-aspect-ratio pointed wings at both subsonic and supersonic speeds. B. Göthert (reference 12) extended the low-aspect-ratio rectangular wing theory of Bollay (references 13 and 14) to include the influence of compressibility and found no effect in the subsonic range. For a very slender inclined body of revolution at subsonic and supersonic speeds, Laitone and Tsien (references 9 and 8) have found that the loading was unaffected by compressibility. That such is also the case for slender inclined, pointed wing-body combinations follows from consideration of the basic differential equation of linearized compressible flow. In addition, it will be shown that the aspect-ratio range to which the theory is applicable becomes larger as the Mach number approaches one.

Prandtl (reference 15) has found the linearized differential equation for the velocity potential of compressible flow to be

$$(1-M_0^2)\frac{\partial^2\varphi}{\partial x^2}+\frac{\partial^2\varphi}{\partial y^2}+\frac{\partial^2\varphi}{\partial z^2}=0 \qquad (24)$$

In the development of the expressions for the forces on long slender wing-body combinations, it has been assumed that $\frac{\partial^2\varphi}{\partial x^2}$ is so much smaller than $\frac{\partial^2\varphi}{\partial y^2}$ and $\frac{\partial^2\varphi}{\partial z^2}$ that the first term of equation (24) may be neglected. Therefore, so long as the term $(1-M_0^2)\frac{\partial^2\varphi}{\partial x^2}$ in the differential equation remains small, Mach number will have little influence on the distribution of the velocity potential. Consequently, Mach number has little effect on the aerodynamic characteristics of a long slender wing-body combination at either subsonic or supersonic speeds. It is immediately apparent that the Mach number cannot be increased indefinitely, for then the coefficient of $\frac{\partial^2\varphi}{\partial x^2}$ becomes so large that the first term will no longer

be negligible. The required condition will be satisfied, however, if the body has a pointed nose, the wing a pointed plan form, and the entire wing-body combination lies near the center of the Mach cone. All these conditions, however, correspond to those originally assumed in the derivation of the expression for the velocity potential (equation (4)). Therefore, the present theory is applicable at supersonic speeds, as well as subsonic speeds, provided the entire wing-body combination lies near the center of the Mach cone.

It has been shown by Robinson and Young (reference 16) that, for finite aspect ratio, the linearized theory of compressible flow (equation (24)) remains theoretically consistent and yields finite and continuous lift-curve slopes in the transonic range. Recent experiments on triangular wings at transonic speeds support this contention by indicating agreement between measured and computed lift-curve slopes. Therefore, to predict the flow around a body traveling at or very near sonic velocity, it is correct, unless the term $\frac{\partial^2\varphi}{\partial x^2}$ becomes extremely large, to let $M_o=1$ and solve the remaining equation for the potential distribution. The remaining equation is the two-dimensional Laplace's equation in the transverse plane. This means that, although the velocity potential may vary in the longitudinal direction, its value at each point may be determined solely by studying the flow in the transverse plane containing the point in question. Therefore, since this is precisely the manner in which the potential distribution was obtained, the results of the present analysis are applicable at transonic speeds. In fact, the present theory is most applicable to wing-body combinations of moderate aspect ratio if the Mach number is one, since it is then no longer necessary to assume that $\frac{\partial^2\varphi}{\partial x^2}$ is very much smaller than $\frac{\partial^2\varphi}{\partial y^2}$ and $\frac{\partial^2\varphi}{\partial z^2}$.

In retrospect, the assumptions related to the study of low-aspect-ratio pointed bodies and the study of moderate-aspect-ratio pointed bodies traveling at sonic speed both lead from the Prandtl equation (equation (24)) to the two-dimensional Laplace's equation in the transverse plane although by different means. The low-aspect-ratio theory neglects the term $(1-M_o^2)\frac{\partial^2\varphi}{\partial x^2}$ in comparison with $\frac{\partial^2\varphi}{\partial y^2}$ and $\frac{\partial^2\varphi}{\partial z^2}$ because $\frac{\partial^2\varphi}{\partial x^2}$ is very small; while the moderate-aspect-ratio sonic theory neglects the same term because $(1-M_o^2)$ is zero.

Thus the determination of the potential distribution for an inclined moderate-aspect-ratio wing at the speed of sound is mathematically equivalent to the determination of the potential distribution of an inclined low-aspect-ratio wing in an incompressible fluid.

EXAMPLES

For a given wing-body configuration complying with the general requirements of the present theory, the load distribution may be determined directly by substituting the proper values for the body radius and wing semispan and their rate of change with x into equations (10) and (11). In addition, closed expressions for the lift, pitching moment, and center-of-pressure position of several elementary configurations may readily be found by simple integration of the integrals indicated by equations (21), (22), and (23). Several such examples will be presented in detail in this section, and the results will be compared in the following section with those obtained from linear theory and from experiment.

Pointed Low-Aspect-Ratio Wing

Although the assumptions of this note have been used previously by R. T. Jones in reference 6 to determine the aerodynamic properties of low-aspect-ratio wings, the load distribution, lift, and pitching moment will be rederived for completeness of presentation and to show a simple application of the preceding expressions. The aerodynamic properties of a low-aspect-ratio wing without fuselage may be determined by letting

$$\frac{a}{s} = 0 \qquad \frac{da}{dx} = 0$$

By substitution of these values into equation (10), it follows that the load distribution along any elemental spanwise strip is

$$\left(\frac{\Delta p}{q}\right)_w = \frac{4\alpha \dfrac{ds}{dx}}{\sqrt{1 - \dfrac{y^2}{s^2}}} \tag{25}$$

The loading (fig. 2(a)) thus shows an infinite peak along the leading edge of the wing. The total load on an elemental spanwise

strip is found from equation (17) to be

$$\frac{d}{dx}\left(\frac{L}{q}\right) q = 4\pi\alpha q s \frac{ds}{dx} \tag{26}$$

Equations (25) and (26) show that the development of lift by the long slender wing depends on an expansion of the sections in a downstream direction. Accordingly, a part of the wing having parallel sides would develop no lift, while a part having contracting width would have negative lift with infinite negative loads along the edges. In the actual flow, however, as R. T. Jones points out (reference 6), the portion of the wing behind the maximum cross section will lie in the viscous or turbulent wake formed over the surface ahead. Consequently, the infinite negative loads will not be developed on these edges. With the aid of the Kutta condition, Jones then concludes that no lift is developed on sections aft of the maximum cross section. This is known to be an oversimplification of the truth and considerable caution should be exercised in applying the present results in the case of constant or gradually contracting width.

The lift coefficient for this wing is found by integration of the load on the elemental strips between the leading edge and the widest section as indicated by substituting equation (26) into equation (21)

$$C_L = \frac{1}{S}\int_0^{c'} 4\pi\alpha s \frac{ds}{dx} dx = \frac{4\pi\alpha}{S}\int_0^{s_{max}} s ds = \frac{\pi}{2}\alpha\frac{4s_{max}^2}{S} = \frac{\pi}{2} A\alpha \tag{27}$$

where c' is the effective wing chord and $\frac{4s_{max}^2}{S} = A$, the aspect ratio. It is seen that the lift-curve slope $\frac{dC_L}{d\alpha}$ depends only on the aspect ratio. It should be noted, however, that the actual lift force depends only on the span and angle of attack and not on the aspect ratio or the area.

By similar substitution and integration by parts of equation (22), the pitching moment about the leading edge is

$$C_m = -\frac{1}{Sc}\int_0^{c'} 4\pi\alpha s \frac{ds}{dx} x dx = -\frac{\pi}{2}\frac{c'}{c}\alpha\left[\frac{4s_{max}^2}{S} - \frac{4(s^2)_m}{S}\right] = -\frac{\pi}{2}\frac{c'}{c} A\alpha\left[1 - \frac{(s^2)_m}{s_{max}^2}\right] \tag{28}$$

where $(s^2)_m = \frac{1}{c'}\int_0^{c'} s^2 dx$ and where moments tending to produce a nosing-up rotation are considered positive. The center-of-pressure location is then found by dividing the moment coefficient by the lift coefficient as indicated in equation (23).

$$\frac{x_{c.p.}}{c} = -\frac{C_m}{C_L} = \frac{c'}{c}\left[1 - \frac{4(s^2)_m}{SA}\right] = \frac{c'}{c}\left[1 - \frac{(s^2)_m}{s_{max}^2}\right] \qquad (29)$$

For a more specific example, consider a triangular wing moving point foremost. Then since $(s^2)_m = \frac{1}{3} s_{max}^2$ and $c'=c$, the pitching-moment coefficient and center-of-pressure position are given, respectively, by $C_m = -\frac{\pi}{3} A\alpha$ and $\frac{x_{c.p.}}{c} = \frac{2}{3}$. The center of pressure is seen to be at the two-thirds chord point or the center of area.

Pointed Slender Body of Revolution

The present method for treating the flow around long slender bodies was introduced by Munk in reference 5 for the determination of the distribution of forces along the longitudinal axis of a body of revolution (airship hull). In the present section, these results will be rederived. In addition, expressions for the total lift, pitching moment, and load distribution will also be presented.

For the slender pointed body of revolution, the following relations exist:

$$\frac{a}{s} = 1 \qquad \frac{da}{dx} = \frac{ds}{dx}$$

where $\frac{da}{dx}$ is not necessarily constant. If these values are substituted into equations (11) and (12), the loading distribution along any elemental strip is

$$\left(\frac{\Delta p}{q}\right)_F = 8\alpha \frac{da}{dx} \sin\theta = 8\alpha \frac{da}{dx}\sqrt{1 - \frac{y^2}{a^2}} \qquad (30)$$

The load distribution (fig. 2(b)) is thus seen to be elliptical, being zero at the extremities of a horizontal diameter and a maximum at the midpoint. The total load on an elemental spanwise strip is found from equation (17) to be

$$\frac{d}{dx}\left(\frac{L}{q}\right) q = 4\pi\alpha q a \frac{da}{dx} = 2\alpha q \frac{dB}{dx} \tag{31}$$

where B is the local cross-section area. It is seen that equation (31) is identical to equation (26) for the integrated load on an elemental spanwise strip of a triangular wing, even though the distribution of load in the two cases is widely different. In contrast, however, to equation (26), which is to be applied only to wings of increasing span, equation (31) may be applied to bodies of revolution in regions of either increasing or decreasing radius, since the Kutta condition does not apply to bodies of revolution. Thus, in general, the lift and pitching moment of a body of revolution are different from those of a wing of identical plan form; however, if the maximum diameter of the body of revolution is at the base station, its lift and pitching moment are equal to those of a wing of identical plan form at the same angle of attack.

As before, the lift coefficient will be determined by substituting equation (31) into equation (21). Taking the area of the base cross section B_b as the reference area and integrating over the length of the body l the lift coefficient is found to be

$$C_L = \frac{1}{B_b}\int_0^l 2\alpha \frac{dB}{dx} dx = 2\alpha \tag{32}$$

since the cross-section area B is B_b at $x=l$ and zero at $x=0$. It is thus seen that the lift of a slender body of revolution depends only on the cross-section area of the base, and is independent of the general shape of the body. A possible effect of viscosity is indicated by such a relationship since the effective base area of the body will be larger than the true base area by an amount dependent on the boundary-layer thickness. Therefore equation (32) will probably tend to underestimate the true lift-curve slope, particularly at lower Reynolds numbers where the boundary-layer thickness is greatest.

By similar substitution and integration by parts, the moment coefficient about the leading edge is

$$C_m = \frac{-1}{B_b l} \int_o^l 2\alpha \frac{dB}{dx} x dx = -2\alpha \left(1 - \frac{B_m}{B_b}\right) \tag{33}$$

where B_m is the mean cross-section area (i.e., the volume of the body divided by the length). The center-of-pressure location is then found through use of equation (23) to be

$$\frac{x_{c.p.}}{l} = -\frac{C_m}{C_L} = 1 - \frac{B_m}{B_b} \tag{34}$$

For a more specific example, consider a cone moving point foremost. The base cross-section area is

$$B_b = \pi a^2$$

The mean cross-section area is

$$B_m = \frac{1}{3} \pi a^2$$

The center of pressure is thus seen to be at the two-thirds point as would be anticipated by the conical nature of the load distribution for this case.

Triangular Wing With Conical Body

The first example of a wing-body combination to be considered is that of a conical body mounted on a triangular wing so that their vertices coincide. The geometry of such a configuration requires that

$$\frac{a}{s} = \frac{da/dx}{ds/dx} = k$$

where both $\frac{da}{dx}$ and $\frac{ds}{dx}$ are constants. If these values are substituted into equations (10) and (11) as described in the two preceding examples, the load distribution along any elemental strip on the wing is given by

$$\left(\frac{\Delta p}{q}\right)_W = 4\alpha \frac{ds}{dx} \left[\frac{1+k^4 - 2k^4 \frac{s^2}{y^2}}{\sqrt{1+k^4 - \frac{y^2}{s^2}\left(1+k^4 \frac{s^4}{y^4}\right)}} \right] \text{for } a \leq y \leq s \tag{35a}$$

and on the body by

$$\left(\frac{\Delta p}{q}\right)_F = 4\alpha \frac{ds}{dx}\sqrt{(1+k^2)^2 - 4\frac{y^2}{s^2}} \quad \text{for } o \leq y \leq a \tag{35b}$$

Figure 2(c) shows the load distribution on a typical wing-body combination of this type together with the load distribution on the same wing without body.

The integrated load on an elemental strip is

$$\frac{d}{dx}\left(\frac{L}{q}\right) q = 4\pi\alpha q s \frac{ds}{dx}\left\{1+k^4+\frac{1}{2\pi}\left[2k(1-k^2)-(1+k^2)^2\sin^{-1}\frac{2k}{1+k^2}\right]\right\} = 4\pi\alpha q s\frac{ds}{dx}(1+R) \tag{36}$$

where

$$R = k^4 + \frac{1}{2\pi}\left[2k(1-k^2)-(1+k^2)^2\sin^{-1}\frac{2k}{1+k^2}\right]$$

The lift coefficient for the entire conical wing-body combination is then

$$C_L = \frac{\pi}{2} A\alpha\,(1+R) = C_{L_W}(1+R) \tag{37}$$

where C_{L_W} is the lift coefficient of the basic triangular wing. The area and aspect ratio of the wing-body configuration are considered to be equal to those of the basic wing. Due to the radial nature of the lines of constant pressure, the center of pressure lies at the two-thirds chord point

$$\frac{x_{c.p.}}{c} = \frac{2}{3} \tag{38}$$

The moment coefficient is then obviously

$$C_m = -\frac{\pi}{3} A\alpha(1+R) = C_{m_W}(1+R) \tag{39}$$

where, similar to before, C_{m_W} represents the pitching moment of the basic wing. Figure 3 shows the variation of $C_{L_\alpha}/C_{L_{\alpha_W}}$ with ratio of body diameter to wing span for this type of wing-body combination. While the wing alone and body alone have identical lift-curve slopes since the widest section is at the trailing-edge, the lift-curve slope of the wing-body combination is always less than that of either a wing or body alone. The maximum loss of

lift-curve slope (about 8 percent) occurs when the body-radius wing-semispan ratio is approximately 0.7.

Triangular Wing on a Semi-Infinite Cylindrical Body

The next example to be considered is that of a triangular wing mounted on a semi-infinite cylindrical body. The essential relationships to be used are that

$$\frac{da}{dx} = 0$$

and that ds/dx is constant. By using these relationships as in the previous examples, it is found that no lift is carried on the body ahead of the leading edge of the root chord. Behind this point, however, lift is carried on both the wing and body and is distributed on any elemental strip of the wing in a manner described by

$$\left(\frac{\Delta p}{q}\right)_W = \frac{4\alpha \frac{ds}{dx}\left(1 - \frac{a^4}{s^4}\right)}{\sqrt{\left(1 + \frac{a^4}{s^4}\right) - \frac{y^2}{s^2}\left(1 + \frac{a^4}{y^4}\right)}} \quad \text{for} \quad a \leq y \leq s \tag{40a}$$

and on the body by

$$\left(\frac{\Delta p}{q}\right)_F = \frac{4\alpha \frac{ds}{dx}\left(1 - \frac{a^4}{s^4}\right)}{\sqrt{\left(1 + \frac{a^2}{s^2}\right)^2 - 4\frac{y^2}{s^2}}} \quad \text{for} \quad o \leq y \leq a \tag{40b}$$

The load distribution at one longitudinal station of a typical wing-body configuration of the type considered in this example is shown in figure 2(d). For purposes of comparison, the load distribution over the same wing without the body is also indicated in figure 2(d).

The integrated load on an elemental strip is given by

$$\frac{d}{dx}\left(\frac{L}{q}\right)_q = 4\pi\alpha q s \frac{ds}{dx}\left(1 - \frac{a^4}{s^4}\right) \tag{41}$$

By integration along the length of the body, the lift coefficient for the complete wing-body combination, based on the area of the basic

triangular wing without fuselage is found to be

$$C_L = \frac{\pi}{2} A\alpha \left(1 - \frac{a^2}{s_{max}^2}\right)^2 = C_{L_W}\left(1 - \frac{a^2}{s_{max}^2}\right)^2 \qquad (42)$$

It may be seen from equation (42) and figure 3 that the addition of a semi-infinite cylindrical body to a triangular wing produces a loss in lift-curve slope just as in the preceding example with the conical body. With the cylindrical body, however, the lift-curve slope has no minimum value, but continues to decrease as the radius-semispan ratio increases until finally, when the latter ratio is one (corresponding to a body without wings), the lift-curve slope is zero. This is as it should be, since a semi-infinite cylindrical body has zero lift-curve slope. The moment coefficient about the vertex of the basic triangular wing is

$$C_m = -\frac{\pi\alpha A}{3}\left(1 - 4\frac{a^3}{s_{max}^3} + 3\frac{a^4}{s_{max}^4}\right) = C_{m_W}\left(1 - 4\frac{a^3}{s_{max}^3} + 3\frac{a^4}{s_{max}^4}\right) \qquad (43)$$

The center-of-pressure position of the complete wing-body combination is given by

$$\frac{x_{c.p.}}{c} = \frac{2}{3} + \frac{4}{3}\left(\frac{\frac{a}{s_{max}}}{1 + \frac{a}{s_{max}}}\right)^2 \qquad (44)$$

Since the center of pressure of the wing alone is at the two-thirds chord point, it may readily be seen the second term of equation (44) represents the change due to the addition of the body. Figure 4 shows the variation of the center-of-pressure position with the ratio of body radius to wing semispan. In contrast to the constant center-of-pressure position of the previous example for the triangular-wing, conical-body combination, the center of pressure of the triangular wing, semi-infinite cylindrical body combination moves rearward as the body radius becomes larger with respect to the wing semispan.

Triangular Wing on a Pointed Body

The case of a triangular wing mounted on a pointed body, closed in an arbitrary manner at the nose but cylindrical along the wing

root chord, may be studied by combining the results of two previous examples. The portion of the wing-body combination ahead of the leading edge of the wing root may be considered to be equivalent to the arbitrary body of revolution treated in the second example. The portion of the wing-body combination aft of the leading edge of the wing root is equivalent to a triangular wing mounted on a semi-infinite cylinder as discussed in the preceding example. The load distribution and the integrated load on any elemental spanwise strip are then the same as those given in the corresponding example.

The lift coefficient is found by adding the lift forces of the component parts of the wing-body combination and dividing by the dynamic pressure q and the characteristic area, again taken to be the area of the basic triangular wing. The lift coefficient is then found to be

$$C_L = \frac{\pi}{2} A\alpha \left(1 - \frac{a^2}{s_{max}^2} + \frac{a^2}{s_{max}^4}\right) = C_{L_W}\left(1 - \frac{a^2}{s_{max}^2} + \frac{a^4}{s_{max}^4}\right) \qquad (45)$$

Figure 3 shows the variation of the lift-curve slope with body-radius wing-semispan ratio. A comparison of the lift-curve slopes shows that the loss in the lift of a triangular wing resulting from the addition of a body having a pointed nose is much less than that resulting from the addition of a semi-infinite body.

The moment coefficient for this wing-body combination may be found in a manner similar to that used in finding the lift coefficient, taking care to transfer the moments of both component parts to the same axis. The moment coefficient about the vertex of the basic triangular wing is

$$C_m = -\frac{\pi\alpha A}{3}\left(1 - 4\frac{a^3}{s_{max}^3} + 3\frac{a^4}{s_{max}^4}\right) - \frac{2\pi\alpha}{S}\left[\frac{a^3}{s_{max}} - \frac{B_m}{\pi}\left(\frac{l}{c} - 1 + \frac{a}{s_{max}}\right)\right]$$

$$= C_{m_W}\left(1 - 4\frac{a^3}{s_{max}^3} + 3\frac{a^4}{s_{max}^4}\right) - \frac{2\pi\alpha}{S}\left[\frac{a^3}{s_{max}} - \frac{B_m}{\pi}\left(\frac{l}{c} - 1 + \frac{a}{s_{max}}\right)\right] \qquad (46)$$

where a represents the radius of the cylindrical portion of the fuselage, l the over-all length of the wing-body combination, and

B_m the mean cross-sectional area (i.e., volume divided by length) of the portion of the body ahead of the leading edge of the wing root.

COMPARISON WITH OTHER RESULTS

As shown in the preceding sections, it is a comparatively simple matter to calculate the load distribution, lift, and center of pressure of complete wing-body configurations by means of the present theory. It has been shown that the theory is most applicable at Mach numbers near one or for configurations having very low-aspect-ratio wings. Its accuracy at other Mach numbers or at larger aspect ratios can best be assessed by comparison with experiment or more nearly exact theory, where available.

Comparisons with available theoretical and experimental lift-curve slopes of triangular wings of varying aspect ratio at supersonic and subsonic speeds are shown in figures 5(a) and 5(b), respectively. In the supersonic range (fig. 5(a)), the linear theory solution of Stewart, Brown, and others (references 17 and 18) for the variation of lift-curve slope with aspect ratio is shown for Mach numbers of 1.0, 1.2, and 1.4. At a Mach number of 1.0, it is seen that the present theory exactly predicts the linear theory value of the lift-curve slopes of triangular wings of any aspect ratio. Increasing the Mach number decreases the degree of correlation at the larger aspect ratios. In summary, this figure indicates that the present theory is very accurate for slender wings at low supersonic speeds where the wing is near the center of the Mach cone, and decreases in accuracy as the wing becomes larger with respect to the Mach cone.

In the subsonic case (fig. 5(b)), no lifting-surface theory for the triangular wing comparable to the supersonic triangular-wing theory exists, and all comparisons will be made directly with experiment. Three test points from reference 19 are shown for wings of aspect ratio 0.5, 1.0, and 2.0 tested at very low Mach and Reynolds numbers in the Langley free-flight tunnel. As in the supersonic case, the accuracy is best at very low aspect ratios and decreases as the aspect ratio increases.

A comparison between lift-curve slopes for a complete wing-body combination consisting of a conical body and a triangular wing calculated by the present theory and by supersonic conical-flow theory is shown in figure 3. A curve presented by Browne, Friedman, and Hodes (reference 20) for the lift-curve slope of a

wing-body configuration consisting of a conical body having a fixed radius of 0.1322 the Mach cone radius and a triangular wing of varying span is shown by the dotted line in figure 3 together with the corresponding curve obtained by the present theory. These two curves never differ by as much as 1 percent, indicating that the present theory and the conical-flow theory are in close agreement in predicting the lift-curve slope at supersonic speeds of a wing-body combination consisting of a slender conical body and a low-aspect-ratio triangular wing.

Ames Aeronautical Laboratory,
National Advisory Committee for Aeronautics,
Moffett Field, Calif.

APPENDIX

Correction to Loading on Portion of Fuselage Aft of Wing Trailing Edge

A method for the calculation of the aerodynamic loading on the entire surface of a slender pointed wing-body combination has been presented based on the assumption that the flow in each transverse plane is independent of that in the adjacent planes. It was noted that the results so obtained were not applicable to the portion of a wing situated behind the widest section because the flow in this region was influenced to a prohibitive degree by the downwash field of the sections further forward. For the same reason, the results are also inapplicable to the portion of the fuselage aft of the wing trailing edge, particularly when the fuselage diameter is small in comparison with the wing span. Since the fuselage is usually extended behind the trailing edge of the wing, it is desirable to determine a correction to apply to the loading expressions.

With assumptions more restrictive than those of the main body of this note, it is possible to obtain an estimate of the corrected loading on the fuselage afterbody. The necessary assumptions are that the downwash velocity in the vicinity of the fuselage with fuselage removed is known, and that the downwash velocity remains constant throughout the entire transverse plane at each longitudinal station. It is immediately apparent that the latter assumption is not entirely correct, but it is true that the downwash velocity is approximately constant over a region of limited lateral extent at

each longitudinal station. Since the forces on a body are produced predominately by the flow field near the body, this assumption should be a valid one as long as the fuselage sections remain in regions of relatively constant downwash velocity in each transverse plane. This means that the fuselage diameter must be small in comparison with the wing span.

With the foregoing assumptions, the loading on the fuselage afterbody may be determined by an extension of the present method. Consider, as in figure 1(a), the flow in the transverse plane as the fuselage afterbody is piercing the $x=x_0$ plane. The flow field corresponding to that of figure 1(b) would then be that of the vertical flow around a circular cylinder. As in the previous analysis, the fuselage radius would, in general, appear to be varying with time. In addition, since the downwash velocity varies with distance behind the wing, the velocity of the vertical flow would also appear to be varying with time. The correct expression for the lift on each strip across the fuselage may then be obtained by substituting the local angle of attack $\alpha-\epsilon$ for the airplane angle of attack α in equation (31) and adding a correction term for the effect of the longitudinal gradient of the downwash velocity. The latter correction term may be determined very simply using the additional apparent mass concept. The correction to the lift force on an elemental strip of unit width across the fuselage afterbody is then given by

$$\Delta \frac{d}{dx}\left(\frac{L}{q}\right) q = m \frac{dw}{dt} = -2Bq \frac{d\epsilon}{dx} \tag{A1}$$

In this equation, the additional apparent mass of a unit length of a circular cylinder of cross-section area B is (see, for instance reference 11, p. 77)

$$m = \rho B \tag{A2}$$

and the vertical velocity in any transverse plane is

$$w = U(\alpha-\epsilon) \tag{A3}$$

where ϵ is the downwash angle. The total lift on each elemental strip of unit width of the fuselage afterbody is then

$$\frac{d}{dx}\left(\frac{L}{q}\right) q = 2q \left[(\alpha-\epsilon) \frac{dB}{dx} - B \frac{d\epsilon}{dx} \right] \tag{A4}$$

Since the downwash angle numerically equals the angle of attack on the wing surface immediately ahead of the wing trailing edge and decreases in value as the distance from the trailing edge increases, it is apparent that ϵ has a positive value and that $\frac{d\epsilon}{dx}$ has a negative value. Thus, effects of downwash angle in equation (A4) tend to cancel each other. Another item which should be mentioned is that the downwash behind wings varies considerably with Mach number. Consequently, compressibility will affect the lift on fuselage afterbodies.

At subsonic speeds, an upwash exists over the portion of the body extending ahead of the wing, although this upwash is of considerably smaller magnitude than the downwash behind the wing for the slender pointed wings considered here. Equation (A4) may be applied to determine the magnitude of the corrected loading taking into account the upwash.

By using methods similar to those developed in the main body of this note rather than the shorter additional apparent-mass methods, it can be shown that the load distribution across each strip of the fuselage afterbody is elliptic.

REFERENCES

1. Lennertz, J.: On the Mutual Reaction of Wings and Body. NACA TM No. 400, 1927.

2. Wieselsberger, C., and Lennertz, J.: Airplane Body (Non Lifting System) Drag and Influence on Lifting System. Influence of the Airplane Body on the Wings. Aerodynamic Theory, vol. IV, div. K, ch. III, W. F. Durand, ed., Julius Springer (Berlin), 1935.

3. Pepper, Perry A.: Minimum Induced Drag in Wing-Fuselage Interference. NACA TN No. 812, 1941.

4. Multhopp, H.: Aerodynamics of the Fuselage. NACA TM No. 1036, 1942.

5. Munk, Max. M.: The Aerodynamic Forces on Airship Hulls. NACA Rep. No. 184, 1924.

6. Jones, Robert T.: Properties of Low-Aspect-Ratio Pointed Wings at Speeds Below and Above the Speed of Sound. NACA TN No. 1032, 1946.

7. Ribner, Herbert S.: The Stability Derivatives of Low-Aspect-Ratio Triangular Wings at Subsonic and Supersonic Speeds. NACA TN No. 1423, 1947.

8. Tsien, Hsue-Shen: Supersonic Flow Over an Inclined Body of Revolution. Jour. Aero. Sci., vol. 5, no. 12, Oct. 1938, pp. 480-483.

9. Laitone, E. V.: The Linearized Subsonic and Supersonic Flow About Inclined Slender Bodies of Revolution. Jour. Aero. Sci., vol. 14, no. 11, Nov. 1947, pp. 631-642.

10. Glauert, H.: The Elements of Aerofoil and Airscrew Theory. Cambridge Univ. Press, 2d ed., 1947.

11. Lamb, Horace: Hydrodynamics. Reprint of sixth ed. (first American ed.), Dover Publications, 1945.

12. Göthert, B.: Plane and Three-Dimensional Flow at High Subsonic Speeds. NACA TM No. 1105, 1946.

13. Bollay, William: A Non-linear Wing Theory and its Application to Rectangular Wings of Small Aspect Ratio. Z.A.M.M., vol. 19, Feb. 1939, pp. 21-35.

14. Bollay, William: A Theory for Rectangular Wings of Small Aspect Ratio. Jour. Aero. Sci., vol. 4, no. 7, May 1937, pp. 294-296.

15. Prandtl, L.: General Considerations on the Flow of Compressible Fluids. NACA TM No. 805, 1936.

16. Robinson, A., and Young, A. D.: Note on the Application of the Linearized Theory for Compressible Flow to Transonic Speeds. College of Aeronautics, Cranfield (Bedfordshire) Rep. No. 2, Jan. 1947.

17. Stewart, H. J.: The Lift of a Delta Wing at Supersonic Speeds. Quart. App. Math., vol. 4, no. 3, Oct. 1946, pp. 246-254.

18. Brown, Clinton E.: Theoretical Lift and Drag of Thin Triangular Wings at Supersonic Speeds. NACA TN No. 1183, 1946.

19. Tosti, Louis P.: Low-Speed Static Stability and Damping-in-Roll Characteristics of Some Swept and Unswept Low-Aspect-Ratio Wings. NACA TN No. 1468, 1947.

20. Browne, S. H., Friedman, L., and Hodes, I.: A Wing Body Problem in Supersonic Conical Flow. Preprint of paper presented at the Inst. Aero. Sci. meeting, Jan. 29, 1948.

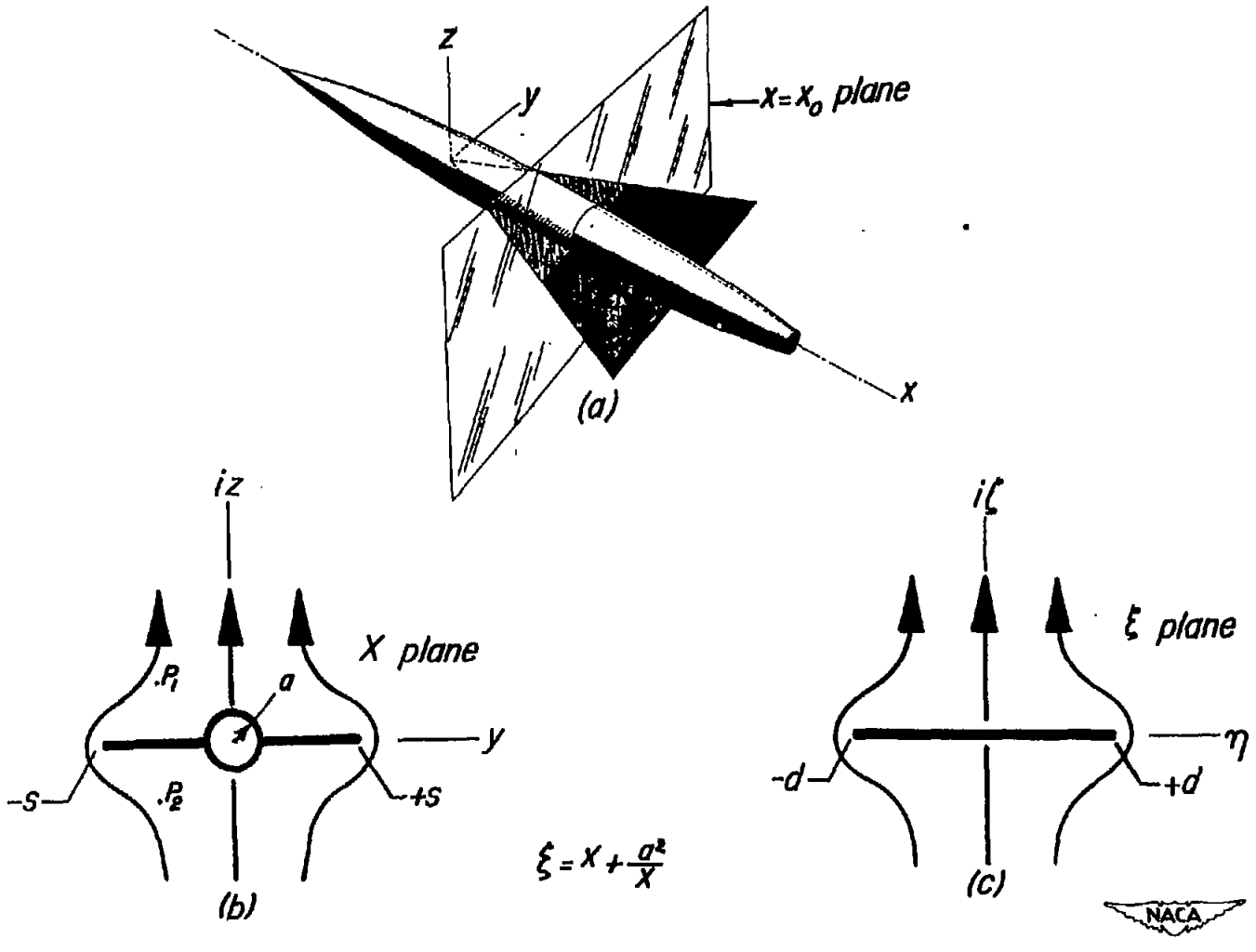

Figure 1.– View of wing-body combination showing coordinate axes and two-dimensional flow fields.

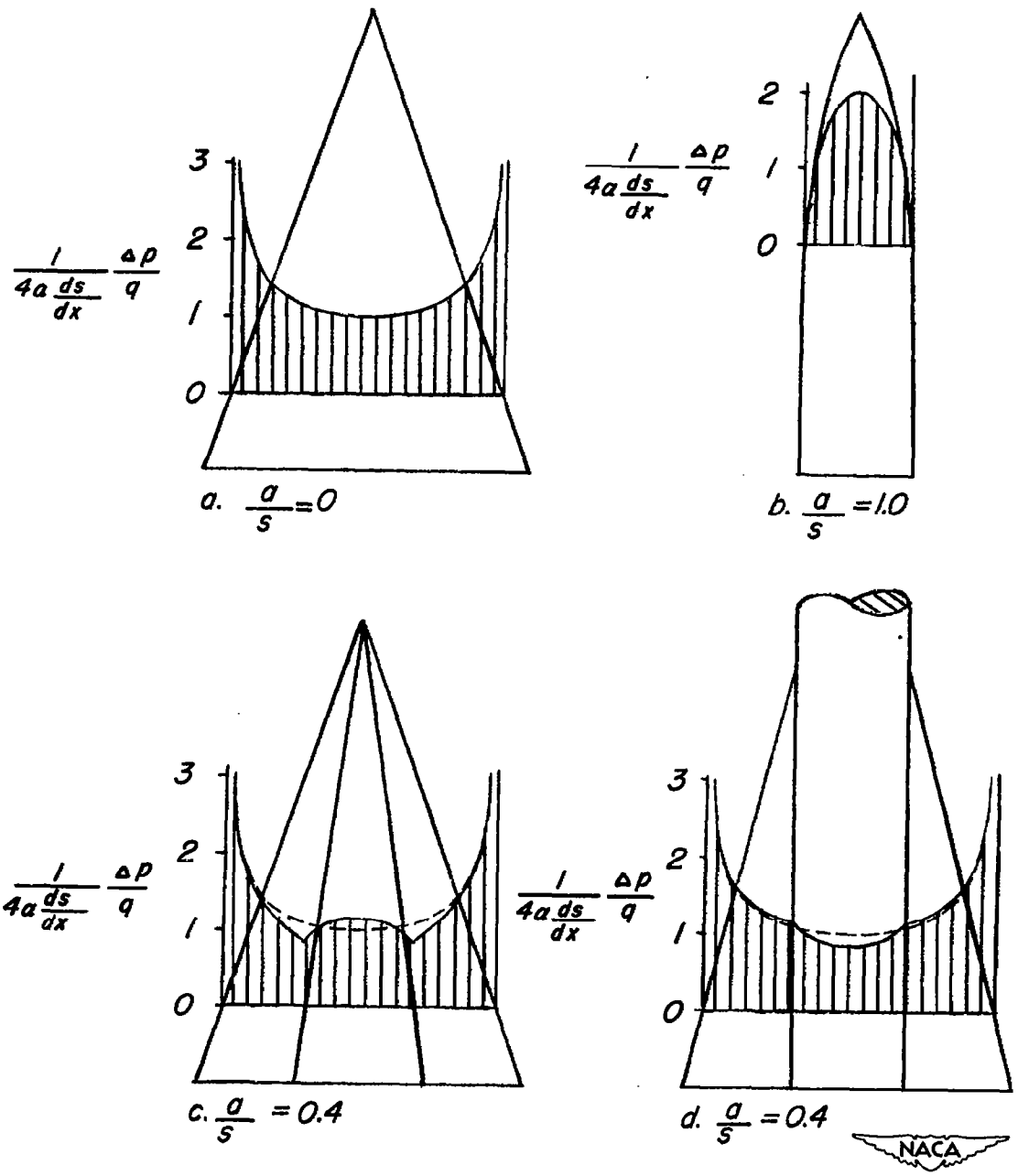

Figure 2.– Load distributions over spanwise sections of four configurations.

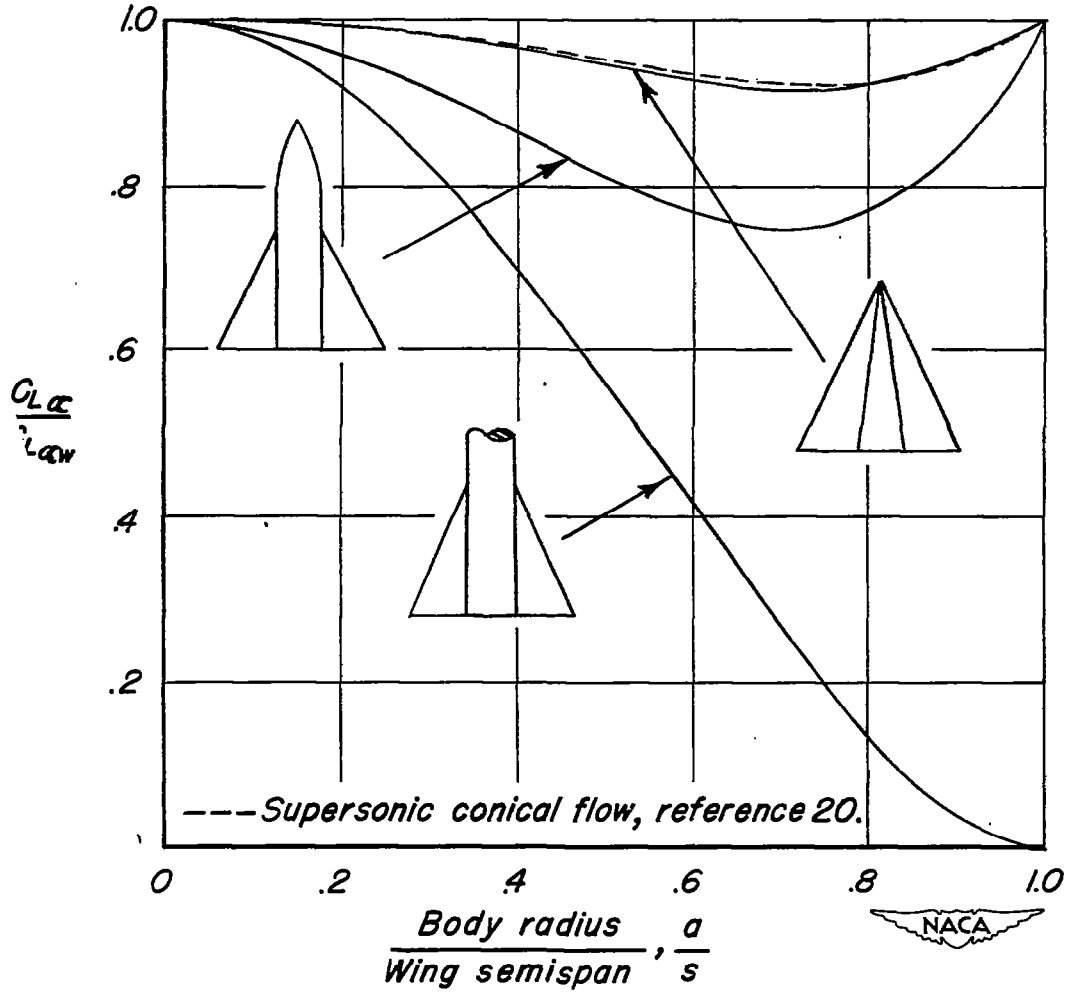

Figure 3.– Lift-curve slope ratios for three wing-body configurations.

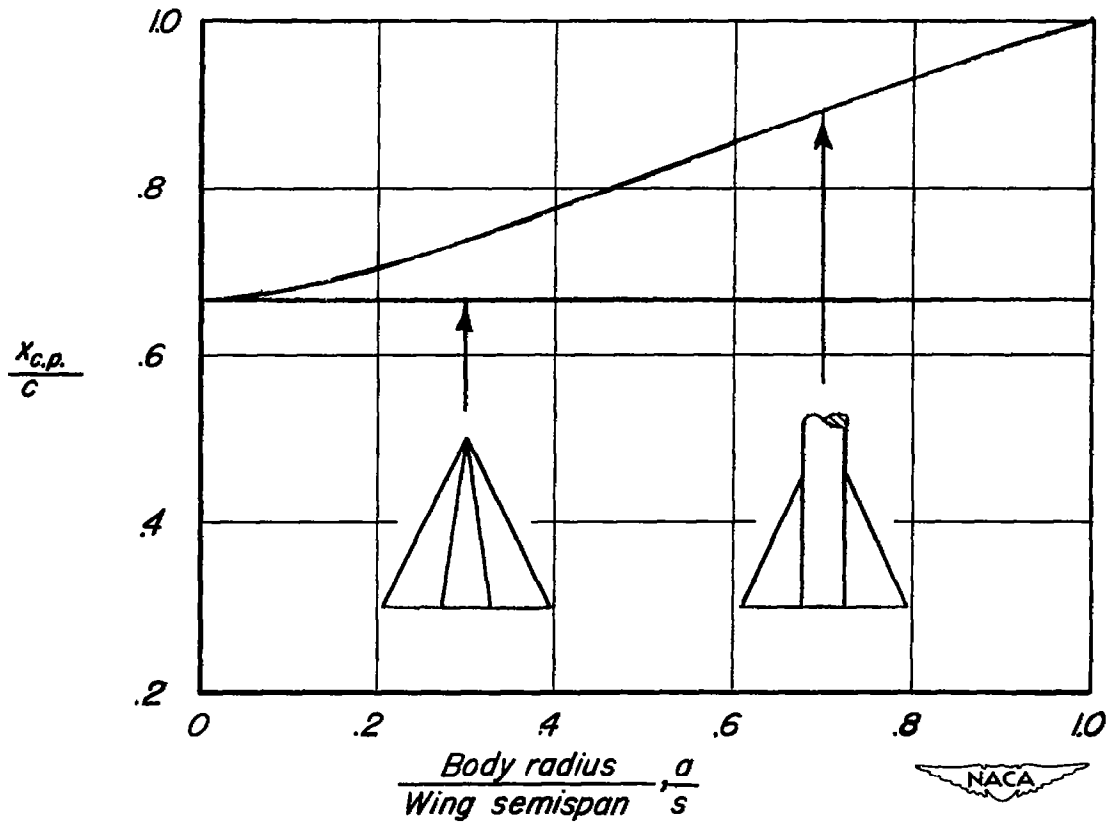

Figure 4.- Center-of-pressure position of two wing-body configurations.

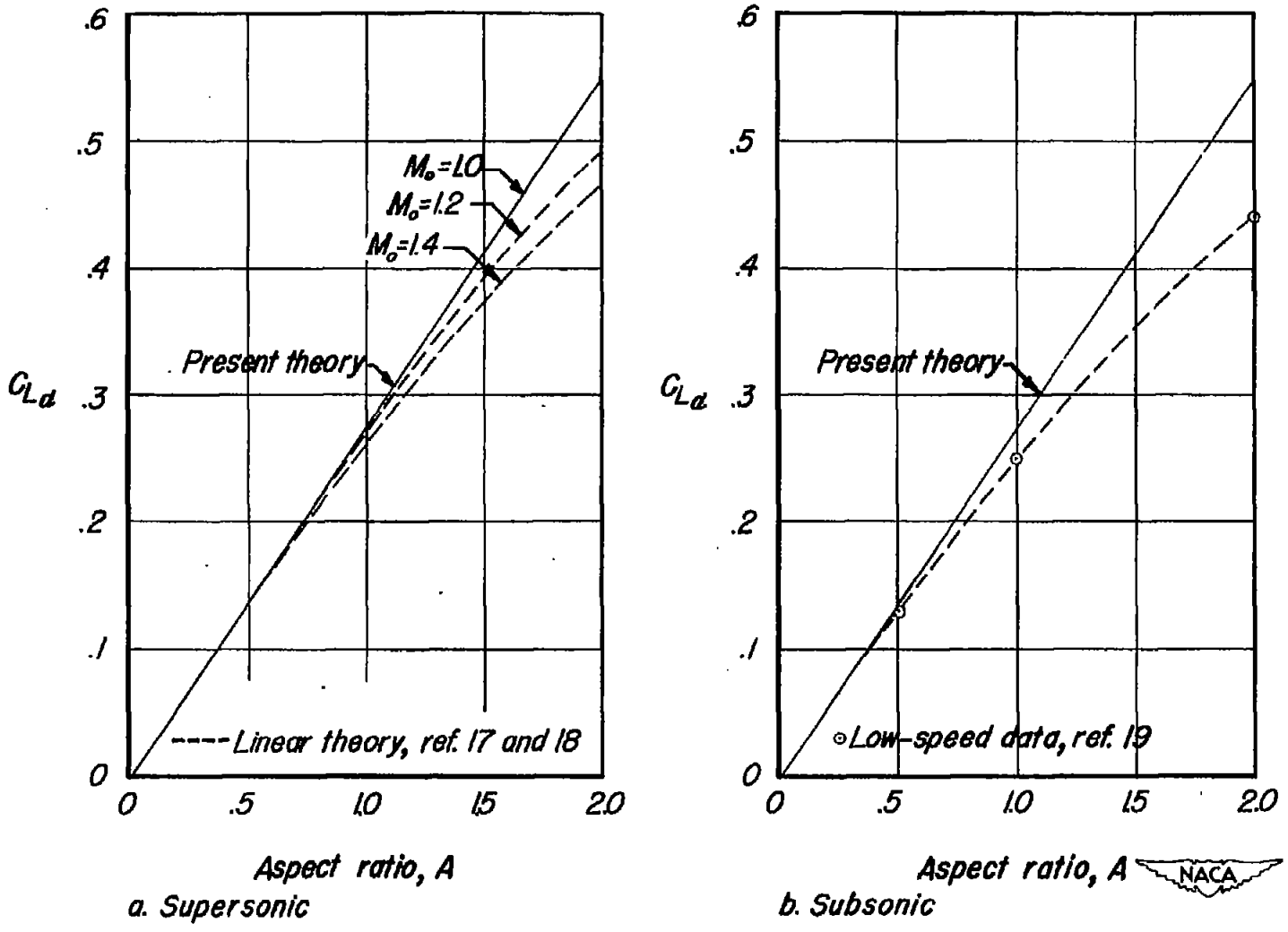

Figure 5.- Comparison of theoretical and experimental lift-curve slopes for triangular wings.